IET Generation, Transmission & Distribution

Research Article

IET Journals
The Institution of Engineering and Technology

Identifying critical risks of cascading failures in power systems

ISSN 1751-8687
Received on 25th May 2018
Revised 13th September 2018
Accepted on 11th April 2019
doi: 10.1049/iet-gtd.2018.5667
www.ietdl.org

Hehong Zhang[1,2], Chao Zhai[3,2], Gaoxi Xiao[3,2] ✉, Tso-Chien Pan[4,2]

[1]*Interdisciplinary Graduate School, Nanyang Technological University, Singapore, Singapore*
[2]*Future Resilient Systems, Singapore-ETH Centre, 1 CREATE WAY, CREATE Tower 138602 Singapore, Singapore*
[3]*School of Electrical and Electronic Engineering, Nanyang Technological University, Singapore, Singapore*
[4]*Institute of Catastrophe Risk Management, Nanyang Technological University, Singapore, Singapore*
✉ *E-mail: egxxiao@ntu.edu.sg*

Abstract: Potential critical risks of cascading failures in power systems can be identified by exposing those critical electrical components on which certain initial disturbances may cause maximum disruption to the systems. The authors investigated the cascading failures in power systems described by the direct current power flow equations, where the initiating disturbances (natural or anthropic factors) give rise to changes in admittances of one or multiple transmission lines. The disruption is quantified with the remaining transmission power at the end of the cascading process. In particular, identifying the critical branches and the corresponding initial disturbances causing the worst-case cascading blackout is formulated as a dynamic optimisation problem (DOP) in the framework of optimal control theory, where the entire propagation process of cascading failures is considered. An Identifying Critical Risk Algorithm based on the maximum principle is proposed to solve the DOP. Simulation results on the IEEE 9-Bus and the IEEE 14-Bus test systems are presented to demonstrate the effectiveness of the algorithm.

1 Introduction

Almost all human systems and activities strongly depend on the steady availability of critical energy infrastructures, e.g. electric power systems. Large-scale power blackout events in history, such as the North America blackout on August 14, 2003 [1], the Europe interconnected grid blackout on November 12, 2006 [2], and the Brazil blackout on November 10, 2009 [3], suggest that power blackouts are not uncommon despite technological advances and great investments on power systems [4]. Large-scale blackouts, once occurred, can lead to huge economic losses or even state panics. Cascading failures in bulk power systems are an important cause of blackouts [5]. A cascading blackout usually starts with one or more initial disturbances that trigger a dramatic redistribution of power flows and consequently some drastic phenomena throughout the power network [6].

Identifying critical risks of cascading failures in power systems is of great interest to researchers and power system planners. Certain disturbances on some components may be responsible for worst power losses or most severe isolations of power systems, making these components the critical components of the systems [7]. To identify the branches and the corresponding initial disturbances, which are associated with the worst-case cascading blackout in power systems, a novel approach within the framework of optimal control theory is proposed in this paper.

A variety of approaches have been proposed to identify critical electrical components and initial attacks or to assess the criticality or vulnerability of power systems. Existing methods typically rely on analysing observed data, and/or conducting numerical simulations adopting various probabilistic, deterministic, approximate, and heuristic approaches [8]. Some of the methods developed for risk assessment of cascading outages are briefly surveyed as follows.

The first class of the existing methods may be conveniently termed as 'detailed modeling and simulation methods', which tend to develop relatively detailed models of system risk. In [9], identifying critical system components (e.g. transmission lines, generators, and transformers) is formulated into a bi-level optimisation model; and a heuristic algorithm is developed to solve the problem and to obtain a local optimal solution. In [10], the problem is recast into a standard mixed-integer linear programming problem, which can be solved by using various solvers. The resulting mixed-integer bi-level programming formulation in [9, 10] is relaxed into an equivalent single-level mixed-integer linear programming problem by replacing the inner optimisation problem with the Karush–Kuhn–Tucker (KKT) optimality conditions [11]. As an extension of [9], a new approach based on 'Global Benders Decomposition' is proposed to solve the large-scale power system interdiction problem when transmission lines are under attacks; and the algorithm can guarantee the convergence of the bi-level optimisation solution [12]. In [13], the vulnerability of power systems under multiple contingencies is formulated as bi-level programming; the upper-level optimisation determines a set of simultaneous outages in the transmission network, whereas the lower-level optimisation models determine the reaction of the system operator against the outages identified in the upper level. In [14], finding a strategic defence to minimise the damages of an attack is formulated as a multi-level mixed-integer programming problem. A Tabu Search with an embedded greedy algorithm is implemented to find the optimum defence strategy. In [15], an improved interdiction model that combines the evaluation of both short-term (seconds to minutes) and medium-term (minutes to days) impacts of possible electric grid attacks to identify the worst one is proposed; an integer programming heuristic is then applied to solve the problem. Power grid performance indices including overall voltage deviation and the minimal load shedding are quantified in [16] based on the alternating current (AC) power flow model, where finding the most disruptive attack is formulated as either a non-linear programming or a non-linear bi-level optimisation problem, both of which can be solved by common algorithms. In [17], both static and dynamic deterministic indices are included in the process of ranking critical nodes; where a new ranking algorithm is proposed and evaluated by extensive Monte Carlo simulations.

The second class of existing methods may be termed as 'bulk analysis methods'. Such methods may be much faster to assess risk since they generally focus on the topological properties of the power networks while largely neglecting the underlying laws of physics and the principles of electrotechnics. Although such 'simplification approaches' certainly help to speed up the

calculations, the simplicity, however, may restrict their accuracy in modelling vulnerabilities in electricity infrastructure [18, 19]. These methods are, therefore, complementary to detailed simulations and provide some useful insights from a different point of view. Therein, the most well-known approach is to identify trends in historical blackout records, where timing and size of past transmission lines outages or demand interruptions are compiled into aggregated measures related to system risk [20]. Another approach is to adopt a complex network-based cascading failure modeling approach, combining the node overload failures and hidden failures of transmission lines in blackouts together [21].

Most of the existing studies have been focusing on identifying the critical components and the initial disturbances that cause a worst-case cascading blackout. In such studies, the problem is usually formulated into a static optimisation problem that neglects the entire propagation process of the cascading failures. Although this makes the problem relatively easier to be solved, the results are sometimes misleading as they may not properly reflect the system dynamics and evolution in the real life.

The main contributions in this paper are two-fold. First, we formulate the task of identifying the critical branches and the corresponding initial disturbances causing the worst-case cascading blackout as a dynamic optimisation problem (DOP) within the framework of optimal control theory. By doing so, we can then examine the entire propagation process of cascading failures. Second, we propose an Identifying Critical Risk Algorithm (ICRA), based on the maximum principle of optimal control theory [22–24], to solve the DOP. This guarantees that the necessary conditions are fulfilled to achieve optimal solutions.

The remainder of this paper is organised as follows. Section 2 formulates the DOP based on the direct current (DC) power flow equations and cascading failure model. In Section 3, the algorithm design based on the maximum principle is introduced in detail. Section 4 presents simulation results based on the IEEE 9-Bus and the IEEE 14-Bus test systems to verify the correctness of the results. Finally, we conclude this work and present some future work in Section 5.

2 Problem formulation

2.1 Notations

The power system notations used in later sections are summarised as follows:

- Number of buses: N_{b}
- Number of transmission branches: N
- Active power at Bus i: P_i
- Active power from Bus i to Bus j: P_{ij}
- Voltage phase at Bus i: θ_i
- Voltage phase difference between Bus i and Bus j: θ_{ij}
- Admittance at Branch i: y_{pi}

The total admittance of a component includes the transformer (if any) and the transmission branch. Related information of a power system can be represented as a component admittance vector $\boldsymbol{Y}_P = [y_{p1} \quad y_{p2} \quad \dots \quad y_{pN}]^{\mathrm{T}}$. The initiating disturbances (natural or anthropic factors) is specified by altering admittance at the corresponding component of $\boldsymbol{Y}_P$. Thereafter, the nodal admittance matrix $\boldsymbol{Y}$ is determined by $\boldsymbol{Y} = \boldsymbol{A}^{\mathrm{T}}\boldsymbol{Y}_P\boldsymbol{A}$, where $\boldsymbol{A}_{N\times N_b}$ is the element-node incidence matrix [25, 26]. In the propagation process of cascading failures, the time-varying component admittance vector $\boldsymbol{Y}_P$ and the time-invariant element-node incidence matrix $\boldsymbol{A}$ are applied to determine the nodal admittance matrix $\boldsymbol{Y}$ for the convenience of analysis.

2.2 DC power flow model

Power flow equations are used to estimate the flow values for each branch within a system. Here, we adopt the DC power flow model as our study is only on high-voltage transmission networks. Adopting this model helps avoid some difficulties in numerical calculations without sacrificing the validity of the results [27].

In the AC power flow model, the active power flow P_{ij} is calculated as

$$P_{ij} = \frac{|U_i||U_j|}{z_{ij}}\sin\theta_{ij} \tag{1}$$

where $|U_i|$ is the voltage amplitude at Bus i and z_{ij} is the component impedance. If one assumes that (i) resistance of the transmission line is ignored, hence line impedance is approximately equal to line reactance; (ii) voltage phase differences are small enough; and (iii) the voltage profile is flat [28], then the non-linear equation above can be linearised into the DC power flow equation.

$$P_{ij} = \frac{\theta_{ij}}{x_{ij}} = y_{ij}\theta_{ij} \tag{2}$$

Furthermore, the power flow equation can be modelled into a matrix format

$$\boldsymbol{P} = \boldsymbol{A}^{\mathrm{T}}\boldsymbol{Y}_P\boldsymbol{A}\boldsymbol{\theta} \tag{3}$$

where $\boldsymbol{P}$ is the vector of active power injections, vector $\boldsymbol{\theta}$ contains the voltage angles at each bus, and $\boldsymbol{A}^{\mathrm{T}}\boldsymbol{Y}_P\boldsymbol{A}$ is the nodal admittance matrix $\boldsymbol{Y}$. Ignoring power loss in the DC power flow equations means that all of the active power injections are known in advance. Once given the nodal admittance matrix, the voltage angles at each bus can be determined by

$$\boldsymbol{\theta} = (\boldsymbol{A}^{\mathrm{T}}\boldsymbol{Y}_P\boldsymbol{A})^{-1}\boldsymbol{P} \tag{4}$$

After the voltage angle value is obtained for each bus, the power flow through each branch can be computed by (2).

2.3 Relay-based overloading branch tripping model

In a power system, transmission branches are protected by circuit breakers. Branch-tripping is one of the most common factors responsible for cascading failures. A circuit breaker trips a transmission branch when the demand load of the branch exceeds a certain threshold level, in order to prevent the transmission branch from being permanently damaged due to overloading [29].

For simplicity, we assume a deterministic model of the mechanism for transmission branch-tripping. In particular, a circuit breaker for branch l_i trips at the moment when the demand load on the branch l_i exceeds its maximum capacity (threshold value). The maximum capacity is defined as the greatest power flow that can be afforded by the branch. This maximum power flow value is decided by thermal, stability, and/or voltage drop constraints. In real-life infrastructures, this value may be constrained by cost as well. The relay-based overloading branch-tripping model is presented as follows, where the threshold value of a branch is related to its initial load

$$C_{\mathrm{tr}1i} = \alpha_i L_i(0) \quad i = 1, 2, \dots, N \tag{5}$$

where $L_i(0)$ is the initial demand load and α_i is the tolerance parameter of line l_i.

The mechanism of the relay protection (above) may be represented by a step function, i.e. when the real load of a branch is less than or equal to the threshold value, its circuit breaker is in the status of on; otherwise, it is in the status off. Derivative calculations are facilitated by introducing a smooth function g that resembles the step function, allowing differentiation of the function at switching points

$$g_i = \begin{cases} 0, & \left|p_{ij}\right| \geq \sqrt{C_{\text{tr1}i}^2 + \dfrac{\pi}{2a}} \\ 1, & \left|p_{ij}\right| \leq \sqrt{C_{\text{tr1}i}^2 - \dfrac{\pi}{2a}} \\ \dfrac{1 - \sin a(\left|p_{ij}^2\right| - C_{\text{tr1}i}^2)}{2}, & \text{otherwise} \end{cases} \tag{6}$$

where $C_{\text{tr1}i} (i = 1, 2, \ldots, N)$ is the threshold value of a branch and a is a parameter to regulate the slope of the function. The returning value of g_i represents the status of a protection relay, where '0' represents that the relay switches off and '1' represents that the relay switches on. Using the smooth function $g_i(p_{ij}, C_{\text{tr1}i})$, the diagonal relay-tripping matrix $\boldsymbol{G}(p_{ij}, C_{\text{tr1}i})$ can be defined as follows:

$$\begin{bmatrix} g_1(p_{ij}, C_{\text{tr11}}) & & & \\ & g_2(p_{ij}, C_{\text{tr12}}) & & \\ & & \ddots & \\ & & & g_N(p_{ij}, C_{\text{tr1}N}) \end{bmatrix}$$

2.4 Cascading failure model

A cascading failure is a sequence of events in which an initial disturbance, or a set of disturbances, triggers a sequence of one or more dependent component outages. Initial disturbances cover a range of exogenous factors, such as high winds, lightning, natural disasters, contact between conductors and vegetation, and human errors, etc. [30]. We assume that the initiating disturbances (natural or anthropic factors) give rise to changes in admittances of certain transmission branches. For example, the outage of a transmission branch due to lightning leads to the infinite impedance or zero admittance between two relevant buses.

Using (6) and the diagonal relay tripping matrix $\boldsymbol{G}(p_{ij}, C_{\text{tr1}i})$, the cascading failure model in matrix format can be built as follows:

$$\boldsymbol{Y}_P^{k+1} = \boldsymbol{G}[P_{ij}^k(\boldsymbol{Y}_P^k), C_{\text{tr1}}]\boldsymbol{Y}_P^k + \text{Diag}[-\boldsymbol{u}(k)]F(\boldsymbol{u}_k) \tag{7}$$

where k is the iterative step of cascading failures and $\boldsymbol{u}(k)$ is the input vector of disturbances. The second term of this equation is used to determine the branch ID, on which the disturbances added can cause more severe damages to a power system through a cascading failure process. The alteration of admittance, ranging from 0 to the original value, has been taken into consideration. Such an alternation includes 'on' and 'off' states of a transmission branch as its special cases. When $k = 0$, the input vector $\boldsymbol{u}(0)$ denotes the initial disturbances. The vector $\boldsymbol{F}(\boldsymbol{u}_k)$ is defined as follows:

$$\boldsymbol{F}(\boldsymbol{u}_{ki}, C_{\text{tr2}i}) = \begin{bmatrix} f_1(\boldsymbol{u}_{k1}, C_{\text{tr21}}) \\ f_2(\boldsymbol{u}_{k2}, C_{\text{tr22}}) \\ \vdots \\ f_N(\boldsymbol{u}_{kN}, C_{\text{tr2}N}) \end{bmatrix}$$

Similar to the purpose of (6), for facilitating derivative calculations, a smooth function $f_i(\boldsymbol{u}_{ki}, C_{\text{tr2}i})$ is applied for every branch of the vector $\boldsymbol{F}(\boldsymbol{u}_k)$. That smooth function is defined as follows:

$$f_i = \begin{cases} 0, & \left|\boldsymbol{u}_{ki}\right| \leq \sqrt{C_{\text{tr2}i}^2 - \dfrac{\pi}{2b}} \\ 1, & \left|\boldsymbol{u}_{ki}\right| \geq \sqrt{C_{\text{tr2}i}^2 + \dfrac{\pi}{2b}} \\ \dfrac{1 + \sin b(\left|\boldsymbol{u}_{ki}^2\right| - C_{\text{tr2}i}^2)}{2}, & \text{otherwise} \end{cases} \tag{8}$$

where C_{tr2} is the threshold value vector and b is a parameter that regulates the slope of the function f. The returning value of the function $f_i(\boldsymbol{u}_{ki}, C_{\text{tr2}i})$ is determined by comparing the threshold value with the corresponding disturbance, where the critical branch identified as the point at which f returns to a value of '1'.

2.5 Dynamic optimisation problem formulation

Based on the models presented above, the DOP formulation in the framework of optimal control theory can be defined as follows:

Formulation of DOP: for a given power system, the control input vector $\boldsymbol{u}_k \in \Omega$ needs to be determined so that the remaining transmission power at the end of the cascading process is minimised. The system is described by the DC power flow equations in (2), and its cascading failure model by (7). Specifically, we have

$$\min_{u_k \in \Omega} J \tag{9}$$

$$J = \left|\left|\boldsymbol{P}^N\right|\right|_F^2 + \epsilon \sum_{k=0}^{N_c - 1} \left(\frac{1}{\max\{0, 1-k\} \max^2\{0, N_n - \left|\left|\boldsymbol{F}(\boldsymbol{u}_k)\right|\right|^2\}} \right) \tag{10}$$

subject to

$$\begin{cases} \boldsymbol{Y}_P^{k+1} = \boldsymbol{G}[P_{ij}^k(\boldsymbol{Y}_P^k), C_{\text{tr1}}]\boldsymbol{Y}_P^k + \text{Diag}[-\boldsymbol{u}(k)]\boldsymbol{F}(u_k) \\ P_{ij} = y_{ij}\theta_{ij} \end{cases} \tag{11}$$

where the Frobenius norm of the power transmission matrix $\left|\left|\boldsymbol{P}^N\right|\right|_F^2$ equals $\sum_{i=1}^N \sum_{j=1}^N (P_{ij}^N)^2$, N_c is the total number of iteration steps in the cascading failures, N_n represents the number of critical branches, $\|\cdot\|$ denotes 2 norm of a vector, and ϵ is the weight-of-cost function. In (10), the terminal constraint $\left|\left|\boldsymbol{P}^N\right|\right|_F^2$ dominates the cost function by setting a sufficiently small weight ϵ.

Remark 1: As discussed earlier, the critical electrical components are those that, when attacked, will trigger a worst-case cascading blackout with the minimum transmission power remaining in the system. Those components and their IDs can be determined by the vector $\boldsymbol{F}(\boldsymbol{u}(k))$ once the optimal control input vector $\boldsymbol{u}(k)$ is obtained.

Remark 2: From the DOP formulation presented above, it can be seen that the disturbances are only applied in the first step ($k = 0$), i.e. the initial disturbance vector $\boldsymbol{u}(0)$. The second term in (10) allows us to add further disturbances (control inputs) to the power grid at the given step of the cascading process. The DOP formulation can be extended to situations where disturbances and/or control inputs can be applied in multiple different steps. For example, during power system cascades, back-up generators may be activated, and excessive loads may be tripped. These can be regarded as adjustments of power flow on certain specific buses. As long as such responses and adjustments are known prior, the adjustments may be taken into account as a part of the time-varying vector of power flow. Under such condition, the status of the branch will be changed due to the flowing power, which will be ultimately reflected in the values of $\boldsymbol{u}(k)$. Note that this may also help facilitate future studies on the roles of human errors in cascading failures and system protections.

3 DOP solution

The DOP can essentially be viewed as a control problem in which one searches for an optimal control input vector $\boldsymbol{u}(k)$ to pin the power grid to the specific worst-case cascading blackout defined in (10). The main principle is to use a tool that indicates the necessary conditions for the optimality of solutions, which helps find the best possible control for driving a dynamical system from one state to another, especially in the presence of constraints of system state or control inputs. The Lagrange multiplier method is widely adopted

with the maximum principle as a strategy for finding the local maxima and minima of a function subject to equality constraints. Therefore, the ICRA based on the maximum principle and the Lagrange multiplier method is developed to solve the DOP presented in (9)–(11). The framework of the algorithm is to solve three equations including adjoint equation, boundary equation, and Hamiltonian equation after introducing Lagrange multipliers for the DOP, to obtain the optimal control input vector $\boldsymbol{u}(k)$. We present the Lagrange multiplier method with the maximum principle in detail below.

The Lagrange multipliers are introduced as $[\lambda_{k+1}] \triangleq [\lambda_1, \ldots, \lambda_N]$, $\lambda_{k+1} \in \mathbb{R}^n$ (usually referred to as adjoint variables) into (9)–(11). The Lagrangian function is as follows:

$$\begin{aligned}\mathfrak{L}(\boldsymbol{Y}_P, \lambda) \triangleq & \parallel \boldsymbol{P}^N(\boldsymbol{Y}_P^N) \parallel_F^2 \\ & + \epsilon \sum_{k=0}^{N_c-1} \left[\frac{1}{\max\{0, 1-k\}} \times \frac{1}{\max^2\{0, N_n - \left|\left|\boldsymbol{F}(\boldsymbol{u}_k)\right|\right|^2\}} \right] \\ & + \lambda_{k+1}^T \left\{ \boldsymbol{G}[P_{ij}^k,\ C_{\text{tr1}}]\boldsymbol{Y}_P^k + \text{Diag}[-\boldsymbol{u}(k)]\boldsymbol{F}(\boldsymbol{u}_k) - \boldsymbol{Y}_P^{k+1} \right\}\end{aligned} \tag{12}$$

where $\lambda \triangleq [\lambda_1^T \quad \lambda_1^T \ldots \quad \lambda_N^T]^{\text{T}}$. To guarantee the existence of the partial derivative $\partial \boldsymbol{Y}_P^{k+1}/\partial \boldsymbol{Y}_P^k$, one must assume that, for each subnetwork that is isolated due to redistributions of power flows in the cascading process, the partial derivative $\partial \boldsymbol{Y}_P^{k+1}/\partial \boldsymbol{Y}_P^k$ is non-singular or reduced-order non-singular on $\mathbb{R}^n \times \Omega$ [29].

Let

$$\boldsymbol{Y}_P^* \triangleq [(\boldsymbol{Y}_0^*)^T \quad \ldots \quad (\boldsymbol{Y}_N^*)^T \quad (\boldsymbol{u}_0^*)^T \quad \ldots \quad (\boldsymbol{u}_{N-1}^*)^T]^{\text{T}}$$

be the vector corresponding to the sequences $[(\boldsymbol{Y}_0^*) \ldots (\boldsymbol{Y}_N^*)]$ and $[\boldsymbol{u}_0^* \ldots \boldsymbol{u}_{N-1}^*]$. Observe that the dual feasibility condition in the KKT conditions is equivalent to the statement that there exists $\lambda^* \triangleq [(\lambda_1^*)^T (\lambda_2^*)^T \ldots (\lambda_N^*)^T]^{\text{T}}$ such that the partial derivative $\partial \mathfrak{L}/\partial \boldsymbol{Y}_P$ of the Lagrangian function vanishes at $(\boldsymbol{Y}_P^*, \lambda^*)$. Therefore, the following conditions hold:

$$\begin{cases} \dfrac{\partial \mathfrak{L}(\boldsymbol{Y}_P^*, \lambda^*)}{\partial \boldsymbol{Y}_P^k} = 0 \\ \dfrac{\partial \mathfrak{L}(\boldsymbol{Y}_P^*, \lambda^*)}{\partial \boldsymbol{u}_k} = 0 \end{cases} \tag{13}$$

where $\partial \mathfrak{L}/\partial \boldsymbol{Y}_P^k$ and $\partial \mathfrak{L}/\partial \boldsymbol{u}_k$ denote the row vectors of partial derivatives:

$$\begin{cases} \dfrac{\partial \mathfrak{L}}{\partial \boldsymbol{Y}_P^k} \triangleq \left[\dfrac{\partial \mathfrak{L}}{\partial \boldsymbol{Y}_{P1}^k} \quad \cdots \quad \dfrac{\partial \mathfrak{L}}{\partial \boldsymbol{Y}_{PN}^k} \right] \\ \dfrac{\partial \mathfrak{L}}{\partial \boldsymbol{u}_k} \triangleq \left[\dfrac{\partial \mathfrak{L}}{\partial \boldsymbol{u}_k^1} \quad \cdots \quad \dfrac{\partial \mathfrak{L}}{\partial \boldsymbol{u}_k^m} \right] \end{cases}$$

To perform the partial differentiation mentioned above, we introduce the Hamiltonian condition, $\mathbb{H}$: $\mathbb{R}^n \times \mathbb{R}^m \times \mathbb{R}^n \to \mathbb{R}$, defined as follows:

$$\begin{aligned}\mathbb{H}(\boldsymbol{Y}_P^k, \boldsymbol{u}_k, \lambda_k) & \\ \triangleq \epsilon \sum_{k=0}^{N_c-1} & \left(\frac{1}{\max\{0, 1-k\} \max^2\{0, N_n - \parallel \boldsymbol{F}(\boldsymbol{u}_k) \parallel^2\}} \right) \\ + \lambda_{k+1}^T & \left\{ \boldsymbol{G}[P_{ij}^k(\boldsymbol{Y}_P^k),\ C_{\text{tr1}}]\boldsymbol{Y}_P^k + \text{Diag}[-\boldsymbol{u}(k)]\boldsymbol{F}(\boldsymbol{u}_k) \right\}\end{aligned} \tag{14}$$

where the first term, $\mathbb{H}$ (denoted as L), is the per-stage weight in the cost function.

We also note that

$$\begin{cases} \dfrac{\partial \mathbb{H}}{\partial \boldsymbol{Y}_P^k} = \dfrac{\partial L}{\partial \boldsymbol{Y}_P^k} + \lambda_k^T \dfrac{\partial \boldsymbol{Y}_P^{k+1}}{\partial \boldsymbol{Y}_P^k} \\ \dfrac{\partial \mathbb{H}}{\partial \boldsymbol{u}_k} = \dfrac{\partial L}{\partial \boldsymbol{u}_k} + \lambda_k^T \dfrac{\partial \boldsymbol{Y}_P^{k+1}}{\partial \boldsymbol{u}_k} \end{cases}$$

where

$$\begin{cases} \dfrac{\partial L}{\partial \boldsymbol{Y}_P^k} \triangleq \left[\dfrac{\partial L}{\partial \boldsymbol{Y}_{P1}^k} \quad \cdots \quad \dfrac{\partial L}{\partial \boldsymbol{Y}_{PN}^k} \right] \\ \dfrac{\partial L}{\partial \boldsymbol{u}_k} \triangleq \left[\dfrac{\partial L}{\partial \boldsymbol{u}_k^1} \quad \cdots \quad \dfrac{\partial L}{\partial \boldsymbol{u}_k^m} \right] \end{cases}$$

Thus, the following conditions hold:

$$\frac{\partial \mathfrak{L}(\boldsymbol{Y}_P^*, \lambda^*)}{\partial \boldsymbol{Y}_P^k} = \frac{\partial \mathbb{H}(\boldsymbol{Y}_P^{k*}, (\boldsymbol{u}_k^*), \lambda_{k+1}^*)}{\partial \boldsymbol{Y}_P^k} - (\lambda_k^*)^T = 0 \tag{15}$$

$$\frac{\partial \mathfrak{L}(\boldsymbol{Y}_P^*, \lambda^*)}{\partial \boldsymbol{Y}_P^N} = \frac{\partial (\left|\left| \boldsymbol{P}^N(\boldsymbol{Y}_P^N) \right|\right|_F^2)}{\partial \boldsymbol{Y}_P^k} - (\lambda_N^*)^T = 0 \tag{16}$$

$$\frac{\partial \mathfrak{L}(\boldsymbol{Y}_P^*, \lambda^*)}{\partial \boldsymbol{u}_k} = \frac{\partial \mathbb{H}(\boldsymbol{Y}_P^{k*}, (\boldsymbol{u}_k^*), \lambda_k^*)}{\partial \boldsymbol{u}_k} = 0 \tag{17}$$

The above conditions together with the cascading failure model in (7) lead to the following equations:

(i) State equations:

$$\boldsymbol{Y}_P^{(k+1)*} = \boldsymbol{G}[P_{ij}^k(\boldsymbol{Y}_P^{k*}),\ C_{\text{tr1}}]\boldsymbol{Y}_P^k + \text{Diag}[-\boldsymbol{u}(k)]\boldsymbol{F}^*(\boldsymbol{u}_k) \tag{18}$$

(ii) Adjoint equations:

$$(\lambda_k^*)^T = \frac{\partial \mathbb{H}(\boldsymbol{Y}_P^{k*}, \boldsymbol{F}^*(u_k), \lambda_{k+1}^*)}{\partial \boldsymbol{Y}_P^k} \tag{19}$$

(iii) Boundary equation:

$$(\lambda_N^*)^T = \frac{\partial (\left|\left| \boldsymbol{P}^N(\boldsymbol{Y}_P^N) \right|\right|_F^2)}{\partial \boldsymbol{Y}_P^N} \tag{20}$$

where the Frobenius norm of transmission power matrix $\left|\left| \boldsymbol{P}^N \right|\right|_F^2$ equals $\sum_{i=1}^N \sum_{j=1}^N (\boldsymbol{P}_{ij}^N)^2$.

(iv) Hamiltonian condition:

$$\frac{\partial \mathbb{H}(\boldsymbol{Y}_P^{k*}, \boldsymbol{u}_k^*, \lambda_{k+1}^*)}{\partial \boldsymbol{u}_k} = 0 \tag{21}$$

For solving (18) through (21), one must address the adjoint equations. From (14) and (19), we obtain the following:

$$\lambda_k^* = \left(\frac{\partial \boldsymbol{Y}_P^{k+1}}{\partial \boldsymbol{Y}_P^k} \right)^{\text{T}} \lambda_{k+1}^* \tag{22}$$

where the dimension of $\partial \boldsymbol{Y}_P^{k+1}/\partial \boldsymbol{Y}_P^k$ is $N \times N$. From (11), we know that each branch of $\boldsymbol{Y}_P^{k+1}$ can be determined by

$$y_{P,i}^{k+1} = g_i(p_{ij}^k,\ C_{\text{tr1}i})y_{P,i}^k + \text{Diag}[-\boldsymbol{u}(k)]_{ii} f_i(\boldsymbol{u}_k) \tag{23}$$

Hence, from (22) and (23), the following partial derivative can be derived:

$$\frac{\partial y_{P,i}^{k+1}}{\partial y_{P,i}^k} = \frac{\partial g_i}{\partial p_{ij}^k} \cdot \frac{\partial p_{ij}^k}{\partial y_{P,is}^k} \cdot y_{P,i}^k + g_i(p_{ij}^k,\ C_{\text{tr1}i}) \tag{24}$$

where $s = 1, 2, \ldots, i, \ldots, N$. The partial derivative of $\partial p_{ij}^k / \partial y_{P,is}^k$ is zero except for when $s = i$. The term $\partial g_i / \partial P_{ij}^k$ equals $-a \cdot p_{ij}^k \cos a(\left|p_{ij}^2\right| - C_{\text{tr1}i}^2)$when p_{ij} satisfies

$$\sqrt{C_{\text{tr1}i}^2 - \frac{\pi}{2a}} \leq \left|p_{ij}\right| \leq \sqrt{C_{\text{tr1}i}^2 + \frac{\pi}{2a}};$$

Otherwise, it becomes equal to zero.

Then we determine the boundary equation. The DC power flow equations are incorporated into the cascading failure model in (7) to express the active power function as follows:

$$\begin{aligned} P_{ij}^k = &(\boldsymbol{A}e_i)^{\mathrm{T}} \mathrm{Diag}(\boldsymbol{Y}_P^k)(\boldsymbol{A}e_j)(e_i - e_j)^{\mathrm{T}} \\ &\cdot [\boldsymbol{A}^{\mathrm{T}} \mathrm{Diag}(\boldsymbol{Y}_P^k)\boldsymbol{A}]^{-1} P \end{aligned} \tag{25}$$

where the vector of the active power P is known for each iterative step. Meanwhile, expression of the active power in the final step can be computed by

$$\begin{aligned} P_{ij}^N = &(\boldsymbol{A}e_i)^{\mathrm{T}} \mathrm{Diag}(\boldsymbol{Y}_P^N)(\boldsymbol{A}e_j)(e_i - e_j)^{\mathrm{T}} \\ &\cdot [\boldsymbol{A}^{\mathrm{T}} \mathrm{Diag}(\boldsymbol{Y}_P^N)\boldsymbol{A}]^{-1} \boldsymbol{P} \end{aligned}$$

From (20) and (25), the following equations are obtained:

$$(\lambda_N^*)^T = \frac{\partial \left[\sum_{i=1}^N \sum_{j=1}^N (\boldsymbol{P}_{ij}^N)\right]^2}{\partial \boldsymbol{Y}_P^N} = \sum_{i=1}^N \sum_{j=1}^N 2P_{ij}^N \frac{\partial p_{ij}^N}{\partial y_P^N} \tag{26}$$

$$\begin{aligned} &\frac{\partial p_{ij}^N}{\partial y_{P,is}^N} \\ &= (\boldsymbol{A}e_i)^{\mathrm{T}} \frac{\partial \mathrm{Diag}(\boldsymbol{Y}_P^N)}{\partial y_{P,is}^N} (\boldsymbol{A}e_j)(e_i - e_j)^T \\ &\cdot [\boldsymbol{A}^{\mathrm{T}} \mathrm{Diag}(\boldsymbol{Y}_P^N)\boldsymbol{A}]^{-1} P + (\boldsymbol{A}e_i)^{\mathrm{T}} \mathrm{Diag}(\boldsymbol{Y}_P^N)(\boldsymbol{A}e_j) \\ &\cdot (e_i - e_j)^T \frac{\partial [\boldsymbol{A}^{\mathrm{T}} \mathrm{Diag}(\boldsymbol{Y}_P^N)\boldsymbol{A}]^{-1}}{\partial y_{P,is}^N} \boldsymbol{P} \end{aligned} \tag{27}$$

For simplicity, the matrix $\boldsymbol{E}_{\mathbf{ii}}$ is used to represent the term $\partial \mathrm{Diag}(\boldsymbol{Y}_P^N)/\partial y_{P,is}^N$. Then (27) can be converted into

$$\begin{aligned} &\frac{\partial p_{ij}^N}{\partial y_{P,is}^N} \\ &= (\boldsymbol{A}e_i)^{\mathrm{T}} \boldsymbol{E}_{\mathbf{ii}} (\boldsymbol{A}e_j)(e_i - e_j)^T [\boldsymbol{A}^{\mathrm{T}} \mathrm{Diag}(\boldsymbol{Y}_P^N)\boldsymbol{A}]^{-1} \boldsymbol{P} \\ &+ (\boldsymbol{A}e_i)^{\mathrm{T}} \mathrm{Diag}(\boldsymbol{Y}_P^N)(\boldsymbol{A}e_j)(e_i - e_j)^T \boldsymbol{P} \\ &\cdot [-\boldsymbol{A}^T \mathrm{Diag}(\boldsymbol{Y}_P^N)\boldsymbol{A}]^{-1} \cdot \boldsymbol{A}^{\mathrm{T}} \boldsymbol{E}_{\mathbf{ii}} \boldsymbol{A} \cdot [\boldsymbol{A}^{\mathrm{T}} \mathrm{Diag}(\boldsymbol{Y}_P^N)\boldsymbol{A}]^{-1} \end{aligned} \tag{28}$$

Finally, we determine the Hamiltonian condition.

$$\begin{aligned} &\epsilon \frac{\partial \left[(1/\max\{0, 1-k\}) \times \left(1/\max^2\left\{0, N_n - \left|\left|\boldsymbol{F}^*(\boldsymbol{u}_k)\right|\right|^2\right\}\right)\right]}{\partial \boldsymbol{u}_k} \\ &+ \frac{\partial [\lambda_{k+1}^T \mathrm{Diag}[-\boldsymbol{u}(k)]\boldsymbol{F}^*(\boldsymbol{u}_k)]}{\partial \boldsymbol{u}_k} = 0 \end{aligned} \tag{29}$$

where $\boldsymbol{F}^*(\boldsymbol{u}_k)$ and $\boldsymbol{u}_k$ are vectors with a $N \times 1$ dimension. The following equations can be acquired according to (29):

$$\begin{aligned} &\frac{4\epsilon}{\max\{0, 1-k\} \times \max^3\left\{0, N_n - \left\|\boldsymbol{F}^*(\boldsymbol{u}_k)\right\|^2\right\}} [\boldsymbol{F}^*(\boldsymbol{u}_k)]^{\mathrm{T}} \\ &\cdot \frac{\partial \boldsymbol{F}^*(\boldsymbol{u}_k)}{\partial \boldsymbol{u}_k} - \lambda_{k+1}^T \left\{\mathrm{Diag}[-\boldsymbol{F}(\boldsymbol{u}(k)] + \frac{\partial \boldsymbol{F}^*(\boldsymbol{u}_k)}{\partial \boldsymbol{u}_k}\right\} = 0 \end{aligned} \tag{30}$$

where the term $\partial \boldsymbol{F}^*(\boldsymbol{u}_k)/\partial \boldsymbol{u}_k$ is given by

$$\frac{\partial \boldsymbol{F}^*(\boldsymbol{u}_k)}{\partial \boldsymbol{u}_k} = \begin{bmatrix} \frac{\partial f^*(\boldsymbol{u}_{k1})}{\partial \boldsymbol{u}_{k1}} & 0 & \cdots & 0 \\ 0 & \frac{\partial f^*(\boldsymbol{u}_{k2})}{\partial \boldsymbol{u}_{k2}} & \cdots & 0 \\ \vdots & \vdots & \ddots & \vdots \\ 0 & 0 & \cdots & \frac{\partial f^*(\boldsymbol{u}_{kn})}{\partial \boldsymbol{u}_{kn}} \end{bmatrix}$$

and the term $\partial f_i^*(\boldsymbol{u}_k)/\partial \boldsymbol{u}_{ki}$ equals $b\boldsymbol{u}_{ki} \cos b(\left|\boldsymbol{u}_{ki}^2\right| - C_{\text{tr2}i}^2)$ when $\boldsymbol{u}_{ki}$ satisfies

$$\sqrt{C_{\text{tr2}i}^2 - \frac{\pi}{2b}} \leq \left|\boldsymbol{u}_{ki}\right| \leq \sqrt{C_{\text{tr2}i}^2 + \frac{\pi}{2b}};$$

Otherwise, it is equal to zero.

Now we can derive the necessary optimality conditions for the control input, which will be the minimisers of the optimisation problem. Using (20) and (22), the recursion formula for the Lagrange multipliers is determined as

$$\lambda_{k+1} = \prod_{s=0}^{N-k-2} \left(\frac{\partial \boldsymbol{Y}_P^{N-s}}{\partial \boldsymbol{Y}_P^{N-s-1}}\right)^T \lambda_N \quad s = 1, 2, \ldots, N-1 \tag{31}$$

The solution of DOP thus can be obtained by solving the following equations:

$$\begin{cases} \frac{4\epsilon}{\max\{0, 1-k\} \times \max^3\left\{0, N_n - \left|\left|\boldsymbol{F}^*(\boldsymbol{u}_k)\right|\right|^2\right\}} \cdot \\ \quad [\boldsymbol{F}(\boldsymbol{u}_k)]^{\mathrm{T}} \frac{\partial \boldsymbol{F}(\boldsymbol{u}_k)}{\partial \boldsymbol{u}_k} - \prod_{s=0}^{N-k-2} \left(\frac{\partial \boldsymbol{Y}_P^{N-s}}{\partial \boldsymbol{Y}_P^{N-s-1}}\right) \lambda_N^T \cdot \\ \quad \left\{\mathrm{Diag}[-\boldsymbol{F}(\boldsymbol{u}(k))] + \frac{\partial \boldsymbol{F}(\boldsymbol{u}_k)}{\partial \boldsymbol{u}_k}\right\} = 0 \\ \boldsymbol{Y}_P^{k+1} = \boldsymbol{G}[P_{ij}^k(\boldsymbol{Y}_P^k),\ C_{\text{tr1}}]\boldsymbol{Y}_P^k + \mathrm{Diag}[-\boldsymbol{u}(k)]\boldsymbol{F}(\boldsymbol{u}_k) \end{cases} \tag{32}$$

where $\boldsymbol{Y}_P^k$ and $\boldsymbol{u}(k)$ are two unknown variables. The algorithm for identifying the critical risks of cascading failures in power systems is summarised in Fig. 1.

As aforementioned, in this study the alteration of the admittance reflecting external disturbances is allowed to vary from 0 all the way to the original admittance value for each branch, which includes 'on' and 'off' states of a transmission branch as its special cases. When it is needed to properly reflect limited effects of certain external disturbances (e.g. temperature, humidity, or ageing problem, etc.), the range of the initiating control action may be restricted to be within a certain range or a few separate limited ranges. Such can be reflected by adding one or multiple linear constraints to the control action, which would not significantly increase the complexity of the algorithm or compromise the effectiveness of the proposed approach. Detailed discussions on such extensions for handling various specific cases, however, are out of the scope of this paper and will be presented in detail in a separate report.

1: Set the maximum step $i_{\max}$, $i = 0$ and $J^* = J_{\min}$
2: **while** $(i \leq i_{\max})$
3: Solve the nonlinear algebraic equations in (32)
4: Determine the control input (external disturbances) $u(k)$
5: Validate the control input $u(k)$ in (7)
6: Compute the resulting cost function J^i in (10)
7: Determine the IDs of critical branches $F(u_k)$ in (8)
8: **if** $(J^i \leq J^*)$
9: Set $u^* = u^i$ and $J^* = J^i$
10: **end if**
11: Set $i = i + 1$
12: **end while**

Fig. 1 *Identifying the Critical Risks Algorithm*

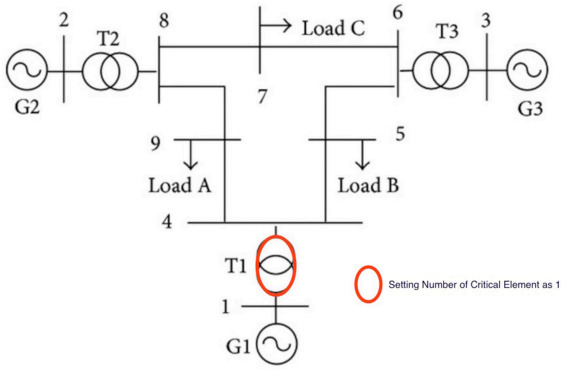

Fig. 2 *Critical branch (marked with a red oval) identified in test case of the IEEE-9 Bus system (for Case 2). Number of critical branches is set as 1*

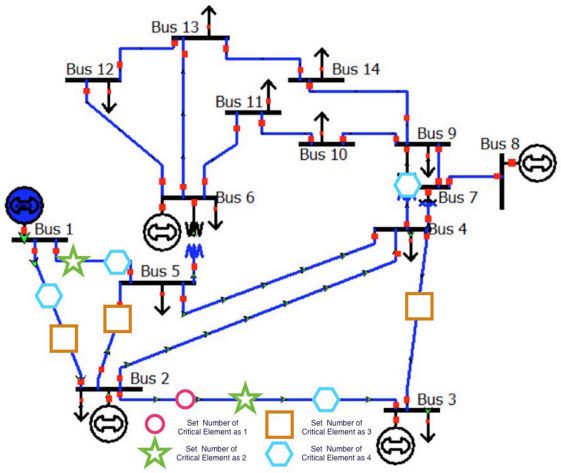

Fig. 3 *Critical branches identified in the test case of the IEEE-14 Bus system (for Case 2), with the number of critical branches set as 1, 2, 3, or 4*

4 Simulation results and verification

We consider two different cases for identifying the critical risks of cascading failures in power systems.

Case 1: Both the critical branches and corresponding initial disturbances are unknown variables.

Case 2: The initial disturbances are given as branch outage where the critical branches remain to be identified. In this case, since the initial disturbances have to be element outages, we replace the vector $\boldsymbol{u}(k)$ in (7) with the initial nodal admittance matrix $\boldsymbol{Y}_P^0$.

Note that *Case* 2 above is a special case of *Case* 1. We are particularly interested in this special case for two reasons: (i) in practice, a branch outage is a common type of failures [31]; and (ii) for this special case, the optimality of the solutions in small or medium-sized systems could be verified by brute force, i.e. by considering all the possible combinations of branch outage cases with a given number of outage branches. In simulations, we use *Matlab* with *fsolve* as the non-linear solvers for solving $\boldsymbol{Y}_P^k$ and $\boldsymbol{u}_k$. For the test case data and calculation of the electric circuit parameters, the codes from Matpower are used extensively.

4.1 Simulation results

The test case of the IEEE 9-Bus system contains three generators, six branches, three loads, and two winding power transformers. The test case of the IEEE 14-Bus system consists of 14 buses, five generators and 11 loads. Information about these two test cases and algorithmic parameters are presented in Table 1. Therein, $\boldsymbol{Y}_{p1} = [-17.36, -10.87, -5.88, -17.06, -9.92, -13.89,$ and $-16.00, -6.21]$
$\boldsymbol{Y}_{p2} = [-16.90, -4.48, -5.05, -5.67, -5.75, -5.85, -23.75, -4.78, -1.80,$

Table 1 Details for two test cases

Information	Test Case 1 (9-Bus)	Test Case 2 (14-Bus)
filename	case9.m	case14.m
nodes	9	14
branches	9	20
iteration No.	10	14
weight ϵ	0.02	0.02
C_{tr2}	$\boldsymbol{Y}_{p1}$	$\boldsymbol{Y}_{p2} - 4E_{14\times 1}$
initial value	$-10 * \text{rand}(N_e, N_c + 1)$	$-9 * \text{rand}(N_e, N_c + 1)$

Table 2 Identification of critical branches and corresponding initial disturbances (for *Case* 1)

	IDs of the critical branches	Initial disturbances, p.u.
9-Bus ($N_n = 1$)	1	17.36
14-Bus ($N_n = 1$)	3	4.73
14-Bus ($N_n = 2$)	2 and 3	4.23 and 4.74

$-3.97, -5.03, -3.91, -7.68, -5.68, -9.09, -11.83, -3.70, -5.21, -5.00, -2.87]$
are the initial susceptance vectors of branches [per-unit (p.u.)] for the 9-Bus and the 14-Bus test systems, respectively. The threshold value vector C_{tr1} for the 9-Bus and the 14-Bus test systems are [0.8, 1.8, 1.0, 0.5, 0.5, 1.0, 0.8, 0.7, 0.5] and [1.8, 1.0, 1.0, 0.8, 0.6, 0.5, 0.9, 0.5, 0.4, 0.7, 0.1, 0.1, 0.3, 0.1, 0.6, 0.1, 0.2, 0.2, 0.1], respectively.

We first perform simulations for *Case* 1. For the IEEE 9-Bus test system, the number of critical branches N_n is set as 1. For the IEEE 14-Bus test system, the number of critical branches N_n is set as 1 or 2. The results are presented in Table 2.

We then conduct simulations for *Case* 2. For the IEEE 9-Bus test system, the number of critical branches N_n is set as 1. The identified critical branch marked with the red oval is shown in Fig. 2. For the IEEE 14-Bus test system, the number of critical branches N_n is set as 1, 2, 3, or 4, respectively. The results are shown in Fig. 3.

4.1 Verification

The correctness of the numerical results generated by the ICRA, as reported in Section 4.1, are verified. For *Case* 1, the computed initial disturbances are applied to the corresponding branches (see Table 2) in each of the test systems. For *Case* 2, the optimality of the solution can be verified by brute force, i.e. by considering all the possible combinations of branch outage cases with a given number of outage branches. For the cascading failure model in (7), we have combined the DC power flow model and relay-based overloading branch tripping model, which is a commonly adopted approach in the state-of-the-art of power systems' cascading failures analysis [27]. The numerical simulation results on the critical branches and disruptive disturbances are validated by disturbing the selected branch with the computed magnitude of disturbances in the corresponding IEEE Bus test systems. Disruptions are quantified according to the final remaining transmission power and/or the final network topology.

For *Case* 1, the IEEE 9-Bus test system, we apply the corresponding initial disturbance, i.e. $u = 17.36$ to Branch 1 connected between Bus 1 and Bus 4. The corresponding initial disturbance $u = 17.36$ equals the outage of Branch 1. The evolution process of transmission network topology is shown in Fig. 4. For the simulation results of *Case* 2, the initial disturbances take the form of branch outage. After testing all the possible branch outage cases, we find that all branches finally are broken when Branch 1 is taken down, which is the same result as that for *Case* 1.

As illustrated in Fig. 4, when the initial disturbance is to break Branch 1, all of the branches finally are broken and the final remaining transmission power is zero. These verification results

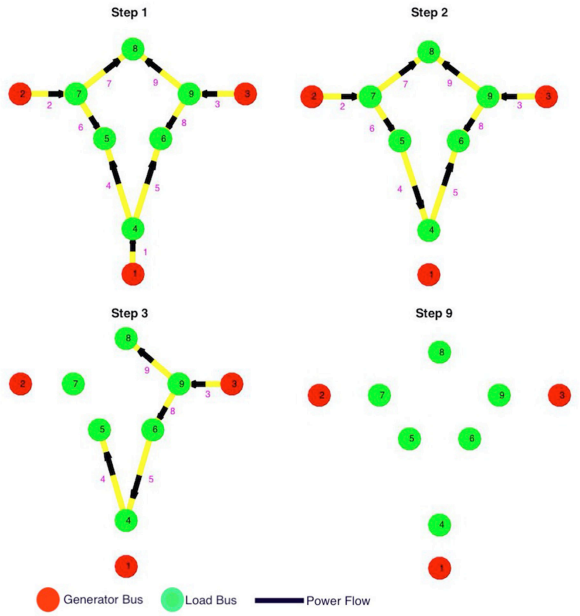

Fig. 4 *Diagram of the propagation process for cascading failure and final power grid topology. Initial disturbance in the IEEE 9-Bus test system is a break in Branch 1*

match with those presented in Table 2 and Fig. 2 and thus verify the correctness of the proposed ICRA.

For the IEEE 14-Bus test system, the initial power transmission is 3.07 p.u. when the power system operates in normal status. For the simulation results of *Case* 1, when the number of critical branches N_n is set as 1, we apply the corresponding initial disturbance, i.e. $u = 4.73$ to Branch 3 connected between Bus 2 and Bus 3. The remaining transmission power is 0.02 p.u. When N_n is set as 2, we apply the initial disturbances $u_2 = 4.23$ and $u_3 = 4.73$ to Branch 2 (connected between Bus 1 and Bus 5) and Branch 3, respectively. The remaining transmission power becomes zero. The simulation results of *Case* 2 involves outages of one, two, three, or four branches that occurs simultaneously with the initial contingencies. A search of all possible scenarios when the number of affected branches varies from one to four produce the results shown in Fig. 5. As displayed in Fig. 5, the outage of Branch 3 is associated with the minimum remaining transmission power, i.e. 0.02 p.u. When $N_n = 2$, the combinations (IDs of branches) [2, 3], [2, 4] and [2, 5] result in zero transmission power. The same outcome is obtained from the combination [1, 5, 6], when $N_n = 3$. When $N_n = 4$, the combinations [1, 2, 3, 9], [1, 2, 3, 10], [1, 2, 3, 11], [1, 2, 3, 12], [1, 2, 3, 13], [2, 4, 6, 7], [2, 4, 6, 8], [2, 4, 6, 9], [2, 4, 6, 10], [2, 4, 6, 11], [2, 4, 6, 12], and [2, 4, 6, 13] lead to zero transmission power. Based on these verification results from *Case* 1 and *Case* 2 above for the IEEE 14-Bus test system, we can confirm that the simulation results presented in Table 2 and Fig. 3 are correct.

Remark 3: It is highly difficult to find an optimal solution for a non-convex optimisation problem, let alone all the optimal solutions with the same objective function value. The proposed method can guarantee to reach a local optimal solution starting from any feasible initial state. By restarting the proposed method from different initial values, we may find multiple suboptimal or even optimal solutions. The offline identification of critical risk, fortunately, allows a large number of restarting operations when such is needed. Note that while no method can guarantee to find all the optimal solutions (except for the brute force method for very small networks) in foreseeable future, identifying any one of the optimal or suboptimal solutions is of value in practice as it may help prevent a certain cascading blackout from happening.

5 Conclusions and future work

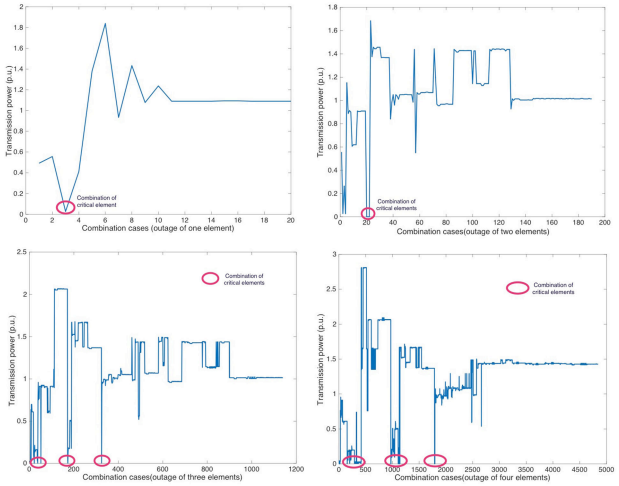

Fig. 5 *Transmission power (in p.u.) remaining when the number of outage branches varies from 1 to 4 in the IEEE 14-Bus test system (for Case 2). Combinations of critical branches are marked with red ovals*

In this paper, the problem of identifying the critical risks of cascading failures in power transmission systems was formulated as a DOP within the framework of optimal control theory. By pinning the power system into the worst-case cascading blackout, the optimal control inputs that reflect the critical branches and the corresponding disturbances were determined by solving the DOP. The ICRA based on the maximum principle was applied to solve the DOP, which provides the necessary conditions for optimality of solutions. The correctness of the ICRA has been verified by applying the computed initial disturbances or branches outage to the corresponding branches in IEEE Bus test systems. The efficient identification of critical risks may help power system planners to reveal hidden catastrophic risks, pre-plan system protection and recovery, and consequently improve system resilience [32]. The research work will be extended to include identifying critical risks as disturbances to network nodes and other mechanisms such as generator tripping, load shedding and voltage collapse, etc. On a long term, we shall take into account the cost of protection and recovery while identifying the worst cases.

6 Acknowledgments

This study is an outcome of the Future Resilient System (FRS) project at the Singapore-ETH Centre (SEC), which is funded by the National Research Foundation of Singapore (NRF) under its Campus for Research Excellence and Technological Enterprise (CREATE) program. Part of this work is also supported by the Ministry of Education (MOE), Singapore, under Contract No. MOE 2016-T2-1-119.

7 References

[1] Liscouski, B., Elliot, W.: 'Final Report on the August 14, 2003 Blackout in the United States and Canada: Causes and recommendations'. A report to US Department of Energy, Washington, DC, 2004, 40

[2] Maas, G.A., Bial, M, Fijalkowski, J.: 'System Disturbance on 4 November 2006'. Final Technical Report, Union for the Coordination of Transmission of Electricity in Europe, 2007

[3] CNN.: 'Dam failure triggers huge blackout in Brazil', 2009

[4] Hines, P., Balasubramaniam, K, Cotilla, S.E.: 'Cascading failures in power grids', *IEEE Potentials*, 2009, **28**, pp. 24–30

[5] Kirschen, D.S., Jayaweera, D.: 'Comparison of risk-based and deterministic security assessments', *IET Gener. Transm. Distrib.*, 2007, **1**, (4), pp. 527–533

[6] Liu, S., Chen, B., Zourntos, T., *et al.*: 'A coordinated multi-switch attack for cascading failures in smart grid', *IEEE Trans. Smart Grid*, 2014, **5**, (3), pp. 1183–1195

[7] Carreras, B.A., Lynch, V.E., Dobson, I., *et al.*: 'Critical points and transitions in an electric power transmission model for cascading failure blackouts', *Chaos Interdiscip. J. Nonlinear Sci.*, 2002, **12**, (4), pp. 985–994

[8] Vaiman, M., Bell, K., Chen, Y., *et al.*: 'Risk assessment of cascading outages: methodologies and challenges', *IEEE Trans. Power Syst.*, 2012, **27**, (2), p. 631

[9] Salmeron, J., Wood, K., Baldick, R.: 'Analysis of electric grid security under terrorist threat', *IEEE Trans. Power Syst.*, 2004, **19**, (2), pp. 905–912

[10] Motto, A.L., Arroyo, J.M., Galiana, F.D.: 'A mixed-integer LP procedure for the analysis of electric grid security under disruptive threat', *IEEE Trans. Power Syst.*, 2005, **20**, (3), pp. 1357–1365
[11] Arroyo, J.M., Galiana, F.D.: 'On the solution of the bilevel programming formulation of the terrorist threat problem', *IEEE Trans. Power Syst.*, 2005, **20**, (2), pp. 789–797
[12] Salmeron, J., Wood, K., Baldick, R.: 'Worst-case interdiction analysis of large-scale electric power grids', *IEEE Trans. Power Syst.*, 2009, **24**, (1), pp. 96–104
[13] Arroyo, J.M.: 'Bilevel programming applied to power system vulnerability analysis under multiple contingencies', *IET Gener. Transm. Distrib.*, 2010, **4**, (2), pp. 178–190
[14] Romero, N., Xu, N., Nozick, L.K., *et al.*: 'Investment planning for electric power systems under terrorist threat', *IEEE Trans. Power Syst.*, 2012, **27**, (1), pp. 108–116
[15] Wang, Y., Baldick, R.: 'Interdiction analysis of electric grids combining cascading outage and medium-term impacts', *IEEE Trans. Power Syst.*, 2014, **29**, (5), pp. 2160–2168
[16] Kim, T., Wright, S.J., Bienstock, D., *et al.*: 'Analyzing vulnerability of power systems with continuous optimization formulations', *IEEE Trans. Netw. Sci. Eng.*, 2016, **3**, (3), pp. 132–146
[17] da Silva, A.M.L., Jardim, J.L., de Lima, L.R., *et al.*: 'A method for ranking critical nodes in power networks including load uncertainties', *IEEE Trans. Power Syst.*, 2016, **31**, (2), pp. 1341–1349
[18] Zhai, C., Zhang, H., Xiao, G., *et al.*: 'Comparing different models for investigating cascading failures in power system'. 2017 Int. Workshop Complex Systems and Networks (IWCSN), Doha, Qatar, 2017, 10.1109/IWCSN.2017.8276532
[19] Hines, P.D., Rezaei, P., Blumsack, S.: 'Do topological models provide good information about electricity infrastructure vulnerability?', *Chaos Interdiscip. J.Nonlinear Sci.*, 2010, **20**, (3), p. 033122-1-033122-6
[20] Carreras, B.A., Newman, D.E., Dobson, I., *et al.*: 'Evidence for self-organized criticality in a time series of electric power system blackouts', *IEEE Trans. Circuits Syst. I*, 2004, **51**, (9), pp. 1733–1740
[21] Wenli, F., Zhigang, L., Ping, H., *et al.*: 'Cascading failure model in power grids using the complex network theory', *IET Gener. Transm. Distrib.*, 2016, **10**, (15), pp. 3940–3949
[22] Sage, A.P., White, C.C.: '*Optimum systems control*' (Prentice Hall, Upper Saddle River, NJ, USA, 1977)
[23] Wang, G., Wu, Z.: 'The maximum principles for stochastic recursive optimal control problems under partial information', *IEEE Trans. Autom. Control*, 2009, **54**, (6), pp. 1230–1242
[24] Yuan, Y., Yuan, H., Wang, Z., *et al.*: 'Optimal control for networked control systems with disturbances: a delta operator approach', *IET Control Theory Appl.*, 2017, **11**, (9), pp. 1325–1332
[25] Perez, L.G., Flechsig, A.J., Venkatasubramanian, V.: 'Modeling the protective system for power system dynamic analysis', *IEEE Trans. Power Syst.*, 1994, **9**, (4), pp. 1963–1973
[26] Knight, U.G.: '*Power systems engineering and mathematics: international series of monographs in electrical engineering*' (Elsevier, Duivendrecht, Netherlands, 2017)
[27] Hines, P.D., Rezaei, P.: 'Cascading failures in power systems', Smart Grid Handbook, (Wiley Online Library, Hoboken, NJ, USA, 2016), pp. 1–20
[28] Purchala, K., Meeus, L., Van Dommelen, D., *et al.*: 'Usefulness of DC power flow for active power flow analysis'. Proc. IEEE Power Engineering Society General Meeting, San Francisco, CA, USA, 2005, pp. 454–459
[29] Song, J., Cotilla-Sanchez, E., Ghanavati, G., *et al.*: 'Dynamic modeling of cascading failure in power systems', *IEEE Trans. Power Syst.*, 2016, **31**, (3), pp. 2085–2095
[30] Eppstein, M.J., Hines, P.D.: 'A 'random chemistry' algorithm for identifying collections of multiple contingencies that initiate cascading failure', *IEEE Trans. Power Syst.*, 2012, **27**, (3), pp. 1698–1705
[31] Stott, B., Jardim, J., Alsac, O.: 'DC power flow revisited', *IEEE Trans. Power Syst.*, 2009, **24**, (3), pp. 1290–1300
[32] Amraee, T., Ranjbar, A.M., Feuillet, R., *et al.*: 'System protection scheme for mitigation of cascaded voltage collapses', *IET Gener. Transm. Distrib.*, 2016, **3**, (3), pp. 242–256